Ultrafast dynamics of soft phonon modes in perovskite dielectrics observed by coherent phonon spectroscopy

Kohmoto, Toshiro

Masui, M

Abe, M

Moriyasu, Takeshi

Tanaka, Koichiro

(Citation)
Physical Review B,83(6):064304-064304

(Issue Date)
2011-02-28

(Resource Type)
journal article

(Version)
Version of Record

(URL)
https://hdl.handle.net/20.500.14094/90001299

Ultrafast dynamics of soft phonon modes in perovskite dielectrics observed by coherent phonon spectroscopy

T. Kohmoto,[1] M. Masui,[1] M. Abe,[1] T. Moriyasu,[1] and K. Tanaka[2]
[1]*Graduate School of Science, Kobe University, Kobe 657-8501, Japan*
[2]*Graduate School of Engineering, Nagoya Institute of Technology, Nagoya 466-8555, Japan*
(Received 16 November 2010; revised manuscript received 14 January 2011; published 28 February 2011)

Coherent phonons were observed in perovskite dielectrics $LaAlO_3$ and $KMnF_3$ using ultrafast polarization spectroscopy. Ultrafast dynamics and softening of phonon modes, which contribute to structural phase transitions, were studied. The temperature dependences of the phonon frequency and relaxation rate were obtained from the observed damped oscillation of coherent phonons. In $LaAlO_3$, typical softening of the phonon frequency was observed toward the phase-transition temperature T_c ($\sim$750 K). The observed relaxation for the soft-mode phonons is explained well by a population decay due to anharmonic phonon-phonon coupling. In $KMnF_3$, two structural phase-transition temperatures, T_{c1} ($=$ 187 K) and T_{cm} ($\sim$81 K), were found through birefringence measurement. At temperatures below T_{cm}, three modes of coherent phonons were observed and the phonon modes were found to undergo softening toward T_{cm}. The observed dependences of the coherent phonon signal on the pumping polarization and the temperature suggest an orthorhombic structure, instead of a monoclinic structure, at temperatures below T_{cm}. The sudden decrease in the phonon frequency at T_{cm} indicates the first-order character of the phase transition at T_{cm}. Notable changes in birefringence and phonon frequency were observed at around 90 K, but no distinct anomaly is found, which suggests that the structure undergoes continuous change. Above 100 K, the E_g mode in the tetragonal symmetry is found to undergo softening toward T_{c1}. A coherent phonon signal of relaxation type appears at around T_{c1} and survives even at near room temperature, which suggests the existence of structural disorder even in the cubic symmetry above T_{c1}.

DOI: 10.1103/PhysRevB.83.064304 PACS number(s): 63.20.dd, 64.70.kp, 78.47.jh, 78.20.Fm

I. INTRODUCTION

Optical information on the dielectric response is usually obtained from the experiments of Raman scattering or infrared spectroscopy. Observation of coherent phonons has also been demonstrated to be very useful for the investigation of low-frequency dielectric response. The time-resolved study of the dynamics of phonons[1] and phonon polaritons[2] was found to be very helpful in determining the properties of the low-frequency optical phonons. At low frequencies, this time-domain technique is very sensitive and provides a very good signal-to-noise ratio as compared to the conventional frequency-domain techniques, in which it is not easy to separate Raman scattering signals from the Rayleigh scattering of excitation laser light in a low-frequency region. At higher frequencies, however, a better performance can be achieved using conventional techniques. Therefore, coherent phonon spectroscopy and conventional frequency-domain techniques can be considered to be complementary methods for the investigation of the dielectric response.

In the case of slight distortion from cubic structure, the intensity of the first-order Raman signal is very small and is of the same order of magnitude as many second-order signals in the experiments of Raman scattering. One such example is $SrTiO_3$ in the low-temperature phase.[3] Even in such a case, background-free signals of the first order can be obtained from the observation of coherent phonons.[4] In the studies on light-illumination effect, it is not easy to separate Raman scattering signals from luminescence. Coherent phonon spectroscopy is not sensitive to the luminescence and is a powerful technique to investigate light-illumination effects as compared to the Raman scattering measurement.[5]

In the present work, ultrafast polarization spectroscopy is used to observe the coherent optical phonons in perovskite dielectrics $LaAlO_3$ and $KMnF_3$, which are generated by femtosecond optical pulses through the process of impulsive stimulated Raman scattering.[6,7] The time-dependent linear birefringence induced by the generated coherent phonons is detected as a change in the polarization of probe pulses. Damped oscillation of coherent phonons is observed, and the temperature dependences of the phonon frequency and relaxation rate are measured. The soft phonon modes related to the structural phase transitions are studied, and we show that the approach in the time domain is very useful for the study on the structural phase transitions and soft phonon modes in dielectric materials.

AMX_3 perovskite structures are one of the largest classes of samples in studies on structural phase transitions. Lanthanum aluminate $LaAlO_3$ is known to undergo a structural phase transition at $T_c \sim 750$ K from cubic space group O_h^1 ($Pm3m$) to rhombohedral D_{3d}^6 ($R\bar{3}c$).[8,9] $LaAlO_3$ was first characterized structurally by Geller and Bala,[10] who found the transformation of the structure from rhombohedral at room temperature to cubic; the transition temperature was later determined by x-ray[11] and electron paramagnetic resonance[12] techniques.

The rhombohedral distortion from the high-temperature cubic structure can be pictured as alternate librations of AlO_6 octahedra. This distortion is similar to the tetragonal distortion occurring in other materials with perovskite structures, such as strontium titanate $SrTiO_3$ ($T_c = 105$ K), which consists of an out-of-phase rotation of adjacent oxygen octahedra in the (100) planes.[9] The oxygen octahedra distort in a manner that can be approximated by a rigid rotation. The rotation in $LaAlO_3$ is about the [111] body-diagonal of the cube, while

that in $SrTiO_3$ is about the [001] crystal axis. Strictly speaking, these are not rigid rotations, since the oxygen ions remain on the cubic faces. This viewpoint was originally proposed by de Rango *et al.*[13] and by Cochran and Zia.[14]

These phase transitions are characterized by the softening of the same optical phonons located at the same point, the $R(1/2,1/2,1/2)$ corner of the cubic Brillouin zone, and the doubling of the unit cell. Since this R mode is triply degenerate in the cubic phase, three independent linear combinations of displacements are possible. These combinations correspond to the rotation-like distortions of oxygen octahedra about the [001], [111], and [110] axes, resulting in tetragonal, rhombohedral, and orthorhombic lattices, respectively, below the phase-transition temperature T_c. The rhombohedral distortion from the cubic symmetry in $LaAlO_3$ corresponds to the condensation of a linear combination of all three cubic components of the R mode, while $SrTiO_3$ has a tetragonal distortion resulting from the condensation of only one of the cubic components of the R mode. Tetragonal distortion occurs in $SrTiO_3$, and rhombohedral distortion occurs in $LaAlO_3$. However, orthorhombic distortion from the cubic symmetry does not occur in nature. Although this distortion is group-theoretically permitted, it does not minimize the free energy and is, therefore, thermodynamically unstable.[15]

In the cubic phase above T_c, all phonon modes are Raman-forbidden. In the rhombohedral phase below T_c, the R point becomes the Γ point of the D_{3d} phase, where the R mode splits into two and Raman-active modes of symmetries A_{1g} (singlet) and E_g (doublet) appear.[16]

In many studies on oxygen perovskites, the fluorine perovskite, $KMnF_3$, has also been studied as one of the interesting materials since the first structural investigation in 1953.[17] Potassium manganese trifluoride ($KMnF_3$) and $LaAlO_3$ have the same perovskite structure, and their structural phase transitions are related to the same rotation of the MnF_6 or AlO_6 octahedra, respectively. However, the behavior of the structural phase transitions in $KMnF_3$ is considerably different from that in $LaAlO_3$. $KMnF_3$ has a cubic structure at room temperature and shows a typical sequence of phase transitions in perovskite systems with the decrease in temperature: cubic $\rightarrow$ tetragonal $\rightarrow$ orthorhombic or monoclinic.[18–37] Three structural phase transitions at about 186 K (T_{c1}), 91 K (T_{c2}), and 82 K (T_{cm}) have been reported. In addition to these structural phase transitions, it is known that $KMnF_3$ shows two magnetic phase transitions at about 88 K (T_N), and 82 K (T_{cm}). Three structural phase transitions were observed at 186.5, 88, and 82 K through x-ray diffraction[34] and at 185, 90, and 83 K through neutron diffraction.[36] Furthermore, three anomalies associated with phase transitions at 186.2, 86.6, and 80.5 K were reported through thermal measurements.[37]

The first transition occurs at T_{c1} = 186 K and corresponds to the softening of the R zone-boundary mode located at the $R(1/2,1/2,1/2)$ corner of the cubic Brillouin zone.[29,35] The high-temperature cubic space group O_h^1 $(Pm3m)$ becomes tetragonal D_{4h}^{18} $(I4/mcm)$ with the tetragonal axis c developing about the axis of rotation of the octahedra ($a/c > 1$), namely, one of the [001] cubic axes.[20,34] The tetragonal phase is characterized by staggered (antiferrodistortive) arrangements of the octahedra in the planes perpendicular to the tetragonal axis, with the phase of rotation alternating between neighboring planes.[38] This transition is slightly of the first order, which shows a small thermal hysteresis of approximately 0.2 K.[24,37] In neutron inelastic scattering experiment,[26] remarkable softening of the two phonon modes corresponding to the R and M points of the zone boundary was observed with the decrease of temperature toward T_{c1}. In Raman scattering experiments,[28,29] two soft modes of the E_g and A_{1g} symmetries coming from the R cubic mode were observed below T_{c1}, and tetragonal symmetry was confirmed.

According to several studies, a structural phase transition appears at $T_{c2} = 91$ K, very close to T_N. This transition is associated with the softening of the M zone-boundary mode located at the $M(1/2,0,1/2)$ point in the cubic Brillouin zone.[29,35] This mode involves distortions of the octahedral planes about the same axis as for the R-point phonon, except that the rotations between adjacent planes were now in phase. As observed in the Raman scattering experiment by Kapusta *et al.*,[35] the transition at T_{c2} is characterized by the appearance of three sharp low-frequency modes below T_{c2} with slight temperature dependence; these three modes do not exhibit a soft-mode behavior. A sudden appearance of several other low-frequency Raman lines with A_g symmetry was also observed. These lines coming from the R and M modes of the cubic phase suggest the first-order character of this phase transition, contrary to the assertion of Hidaka *et al.*,[30] who attributed a second-order character to this transition. In the x-ray diffraction experiments[34] and thermal measurements,[37] however, no transition was observed at 91 K.

At $T_N = 88$ K, both M-point condensation and antiferromagnetic transition occur.[24,30,34,37] The R mode condensates about the [001] axis, the M mode condensates about the [110] direction, and the resulting structure is orthorhombic. Simultaneously, an antiferromagnetic ordering of the Mn^{2+} spin network appears. At this temperature, a paramagnetic-to-antiferromagnetic phase transition is superimposed on the tetragonal-to-orthorhombic structural phase transition. As is characteristic of a second-order phase transition, a λ-shaped temperature dependence and no hysteresis have been found in the thermal measurements.[37]

Finally, below $T_{cm} = 82$ K, an orthorhombic or monoclinic phase is developed, in which the octahedra are rotated about all the directions of the cubic phase. At this temperature, characteristic of a first-order phase transition, an abrupt jump and a large hysteresis of approximately 2 K appear in various measurements.[21,30,34,37] These results are consistent with the neutron diffraction measurements,[36] which demonstrate that this transition is structurally of the first order and magnetically of the second order.

As for the magnetic properties, $KMnF_3$ becomes antiferromagnetic below $T_N = 88$ K with a uniaxial spin structure and transforms further to a canted antiferromagnet below $T_{cm} =$ 82 K with a weak spontaneous magnetization.[21,30]

Several studies on structural and magnetic phase transitions have thus far been conducted using various experimental techniques, and it is known that $KMnF_3$ has four phase-transition temperatures: T_{c1}, T_{c2}, T_N, and T_{cm}. However, there are certain discrepancies in their reports. No study has clearly confirmed all four transition temperatures at the same time.

The structural phase transition at $T_{c2} = 91$ K was particularly confirmed by several authors,[24,27,29,30,35] but other authors have claimed that no anomaly is found at T_{c2}.[34,37] This transition was claimed to be either of the first order[24,27,29,35] or of the second order.[30] The transition at $T_N = 88$ K was concluded to be of the first order by some authors[28,34] and of the second order by other authors.[27,30,37] Different candidates for the structure of the low-temperature phase below T_{cm} have been proposed: orthorhombic[20,23,29] and monoclinic.[18,28,35] The results of the structure of the low-temperature phase and the mechanism of the T_{c2} and T_N phase transitions in different studies have long been contradictory. However, no definitive consensus has been obtained yet.

In the present paper, the softening of the tetragonal E_g mode below T_c in $LaAlO_3$ is studied and the mechanism of the phonon relaxation is discussed using a population decay model; in this model, an optical phonon decays into two acoustic phonons due to anharmonic phonon-phonon coupling. In $KMnF_3$, the phase-transition temperatures are investigated by birefringence measurement. The phonon frequencies are obtained from the observed coherent phonon signals, and their behavior near the phase-transition temperatures is studied. The coherent phonon signal of relaxation type is also found around T_{c1}. We discuss the low-temperature symmetry below T_{cm} from the observed dependences of the coherent phonon signal on the pumping polarization and the temperature.

II. EXPERIMENT

Coherent phonons and their softening observed in the time domain are studied by ultrafast polarization spectroscopy with the pump-probe technique. The pump pulse is provided by a Ti:sapphire regenerative amplifier, and the probe pulse by an optical parametric amplifier. The linearly polarized pump and probe beams are nearly collinear and focused on the sample in a temperature-controlled refrigerator or a heated metal block. The waist size of the beams at the sample is approximately 0.1 mm. The wavelength, pulse energy, and pulse width at the sample are 790 nm, $\sim$2 μJ, and 0.2 ps, respectively, for the pump pulse, and 700 nm, $\sim$0.1 μJ, and 0.2 ps for the probe pulse. The repetition rate of the pulses is 1 kHz.

Coherent phonons are generated by the pump pulse through the process of impulsive stimulated Raman scattering, and they induce time-dependent anisotropy of the refractive index. The anisotropy of the refractive index, the linear birefringence, induced by the generated coherent phonons is detected by a polarimeter[39–41] with a quarter-wave plate as a change in the polarization of the probe pulse, whose plane of polarization is tilted by 45° from that of the pump pulse.

The time evolution of the signal was observed by changing the optical delay between the pump and probe pulses. To improve the signal-to-noise ratio, the direction of the linear polarization of the pump pulse was switched with each shot using a photoelastic modulator and a quarter-wave plate; the output signal from the polarimeter was lock-in detected.

For birefringence measurement, we used only the probe pulse. The change in birefringence is detected as a change in the polarization of a linearly polarized probe light.

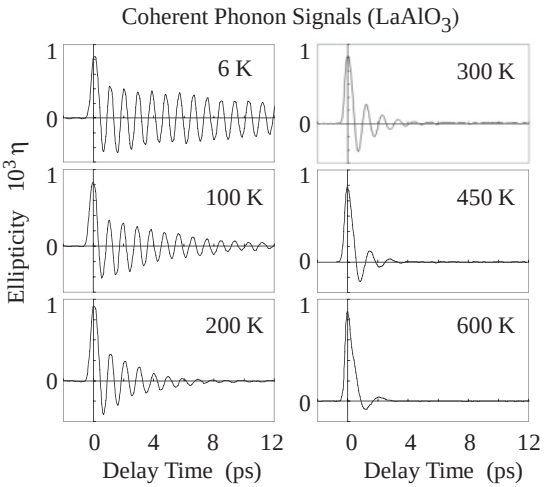

FIG. 1. Damped oscillation of coherent phonons observed in $LaAlO_3$ at 6, 100, 200, 300, 450, and 600 K. The vertical axis represents the ellipticity η in the electric-field amplitude of the transmitted probe pulse.

III. RESULTS

A. Coherent phonons in $LaAlO_3$

Figure 1 shows the damped oscillation of coherent phonons observed in $LaAlO_3$ at 6, 100, 200, 300, 450, and 600 K. The thickness of the sample is 0.2 mm. The direction of the laser beams is perpendicular to the (001) surface, and the polarization direction of the pump pulse is parallel to the [100] axis of the crystal. The vertical axis in Fig. 1 represents the ellipticity η in the electric-field amplitude of the transmitted probe pulse, which is defined by $\eta = (E_+ - E_-)/(E_+ + E_-)$ with circularly polarized field components E_+ and E_-. The induced ellipticity of the probe pulse corresponding to the oscillation amplitude of the coherent phonon signal is $\sim 10^{-3}$. The oscillation period and relaxation time of the coherent phonons at 6 K are 0.9 and 14 ps. As the temperature is increased, the oscillation period becomes longer and the relaxation time becomes shorter. Above T_c, the oscillation disappears. The Fourier transform of the coherent phonon

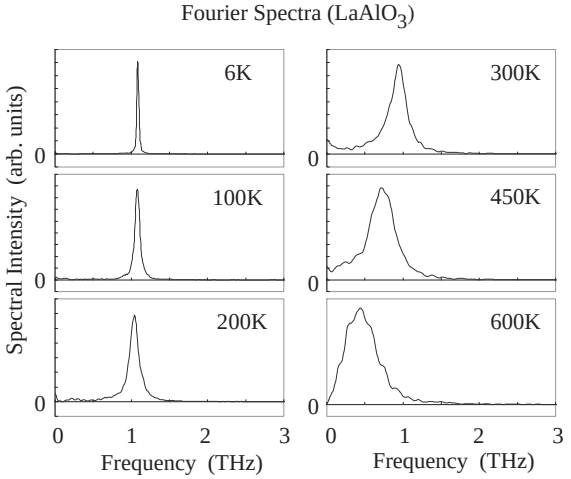

FIG. 2. Fourier transform of the coherent phonon signals in Fig. 1.

signals in Fig. 1 is shown in Fig. 2. At 6 K, a single peak appears at the oscillation frequency of 1.1 THz. As the temperature is increased, the oscillation frequency becomes smaller and the spectral width becomes broader, which corresponds to the shorter relaxation time.

B. Birefringence and coherent phonons in $KMnF_3$

$LaAlO_3$ has a single phase-transition temperature and shows a relatively simple behavior of the coherent phonons. $KMnF_3$, on the other hand, has several phase-transition temperatures and is expected to show a more complicated behavior. Therefore, we measured the temperature dependence of birefringence in $KMnF_3$ before the observation of the coherent phonons. The temperature dependence of the change in birefringence in $KMnF_3$ is shown in Fig. 3, where the polarization plane of the probe light is along the [100] axis and the temperature is decreased. From the change in birefringence in Fig. 3, we can find two clear anomalies at 187 K (T_{c1}) and 81 K (T_{cm}). The phase transition at 81 K has a hysteresis of approximately 2 K, which is consistent with the result of the x-ray diffraction experiment[34] and thermal[37] measurements. A large change in birefringence appears at around 90 K; however, no distinct anomaly is found at T_{c2} and T_N in our birefringence measurement.

Figure 4 shows the coherent phonon signals observed in $KMnF_3$ at 6 K, where the laser beams are perpendicular to the (001) surface and the pump polarization is parallel to the [100] and [110] axes. The thickness of the sample is 0.7 mm. The vertical axis in Fig. 4(a) represents the ellipticity η in the electric-field amplitude of the transmitted probe pulse. At zero delay, a large signal appears due to electronic response; the width of this signal is determined by the pulse width. Next, the damped oscillation of coherent phonons is observed, as shown in Fig. 4(a). The change in the polarization of the oscillation amplitude of the coherent phonon signal is 5×10^{-4} of the electric-field amplitude of the probe pulse, which corresponds to the change $\Delta n \sim 10^{-7}$ of refractive index. In our detection system, a polarization change of $\sim 10^{-5}$ in the electric-field amplitude can be detected.

The oscillation signal for [100] pumping is a simple oscillation with mostly a single frequency, while that for [110] pumping is not a single frequency oscillation. The relaxation times of the coherent phonons at 6 K are 70 ps for [100] pumping and 35 ps for [110] pumping. The Fourier transform of the coherent phonon signals in Fig. 4(a) is shown in Fig. 4(b). Three phonon frequencies, 0.8, 1.2, and 1.5 THz, contribute to the coherent phonon signals. The Fourier spectra indicate that the dominant contributions to the signals are 1.2 THz for [100] pumping and 0.8 and 1.5 THz for [110] pumping.

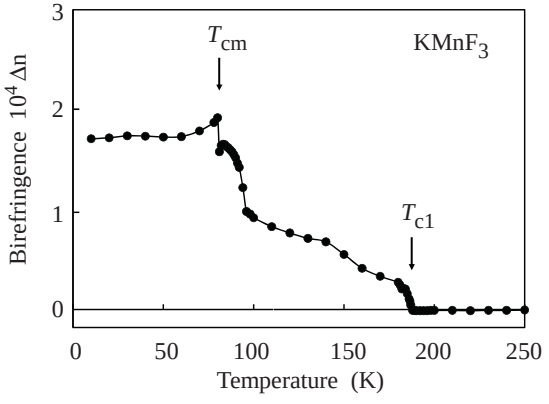

FIG. 3. Temperature dependence of the change in birefringence in $KMnF_3$. The polarization plane of the probe light is along the [100] axis. The temperature was decreased.

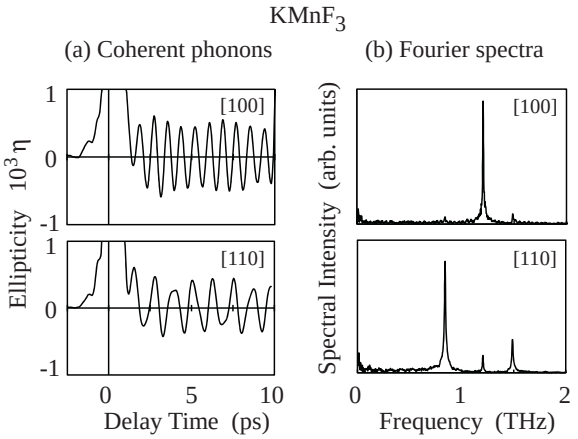

FIG. 4. (a) Coherent phonon signals observed in $KMnF_3$ at 6 K. The laser beams are perpendicular to the (001) surface, and the pump polarization is parallel to the [100] and [110] axes. The vertical axis represents the ellipticity η in the electric-field amplitude of the transmitted probe pulse. (b) Fourier transform of the coherent phonon signals in (a).

The temperature dependence of the coherent phonon signal in $KMnF_3$ observed below 80 K for [100] and [110] pumping is shown in Fig. 5. As the temperature is increased, the oscillation period becomes slightly longer and the relaxation time becomes shorter. The lengthening of the period is more clearly observed for [110] pumping than [100] pumping.

The coherent phonon signals at higher temperatures are shown in Fig. 6 for [100] pumping and in Fig. 7 for [110] pumping. In the coherent phonon experiment, the temperature was increased. The coherent phonon signals above 82 K exhibit various behaviors, while the behavior of those below 80 K in Fig. 5 is relatively simple. In general, phonon modes are classified as either oscillation type or relaxation type. [42] The signal of relaxation type appears around the phase-transition temperature T_{c1} for [100] pumping, as shown in Fig. 6. This signal survives even at near room temperature. For [110] pumping, the signal of oscillation type appears from low temperatures to the phase-transition temperature T_{c1}. However, the period of oscillation becomes longer between 83 and 100 K. At 100 K, the value of the period becomes similar to that at 80 K, after which it monotonously becomes smaller as the temperature is increased.

IV. DISCUSSION

A. $LaAlO_3$

The coherent phonon signal $S(t)$ observed in $LaAlO_3$ is expressed well by damped oscillation $S(t =) A\ e^{-\gamma t} \sin \omega t$, where ω is the oscillation frequency and γ is the relaxation

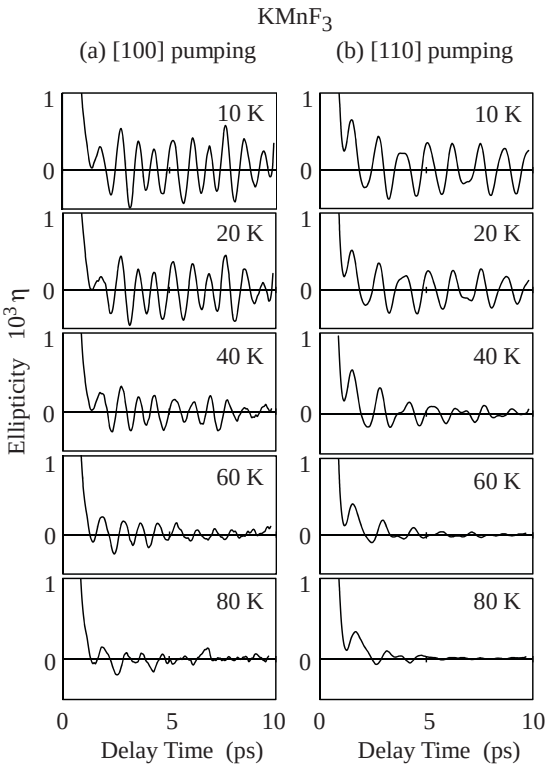

FIG. 5. Temperature dependence of the coherent phonon signal in $KMnF_3$ observed below 80 K for (a) [100] and (b) [110] pumping.

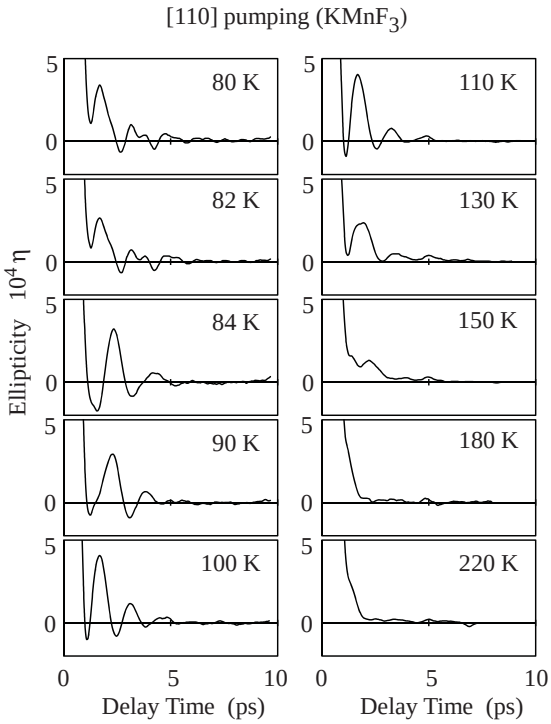

FIG. 7. Temperature dependence of the coherent phonon signal for [110] pumping observed above 80 K. A signal of oscillation type appears from low temperatures to the phase-transition temperature T_{c1}.

rate. This sine-type function is expected for phonons induced by impulsive stimulated Raman scattering.[6,7] The solid circles in Fig. 8 denote the temperature dependence of the oscillation frequency obtained from the coherent phonon signal observed in $LaAlO_3$. As the temperature is increased from 6 K, the oscillation frequency decreases and approaches zero at the phase-transition temperature T_c. This result is consistent with the temperature dependence of phonon frequency for the

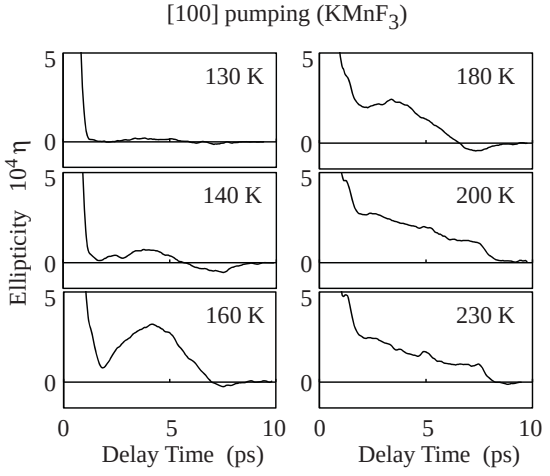

FIG. 6. Temperature dependence of the coherent phonon signal for [100] pumping observed between 130 and 230 K. A signal of relaxation type appears at around the phase-transition temperature T_{c1} and survives even at near room temperature.

E_g mode observed by the Raman scattering experiment.[16] The solid curve describes the temperature dependence of the form $\omega \propto (T_c - T)^n$. The experimental results for the temperature region between 200 K and T_c are explained well by $n = 0.5$, while those below 200 K deviate from that form. According to a simple classical consideration, the relation $\omega^2 \propto (T_c - T)$ is expected from the Lydanne-Sachs-Teller relation and the Curie-Weiss law. The obtained value of n in our experiment is consistent with that consideration.

In the study on structural phase transitions and related soft phonon modes, the frequency of the soft modes becomes small near the phase-transition temperature. After this, it is not easy to separate Raman scattering signals from the background of the Rayleigh scattering of the excitation laser light, and reliable information on the center frequency and the relaxation, or the spectral width is not necessarily obtained from the study on Raman scattering.[3,16] On the other hand, by the present method of coherent phonon spectroscopy in the time domain, background-free damped oscillation can be observed directly and the oscillation frequency and relaxation rate can be obtained accurately.[43]

The solid circles in Fig. 9 denote the temperature dependence of the relaxation rate obtained from the coherent phonon signal for the E_g mode observed in $LaAlO_3$. The relaxation rates increase with the temperature.

In general, the relaxation of coherent phonons is determined by population decay (inelastic scattering) and pure dephasing (elastic scattering). In metals, the pure dephasing due to electron-phonon scattering, which depends on hot electron density, contributes to the phonon relaxation.[44] In dielectric

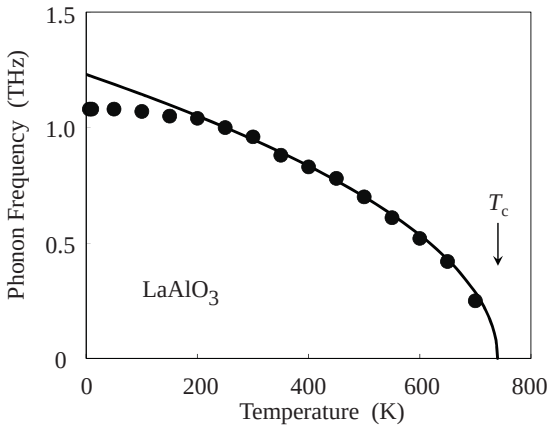

FIG. 8. Temperature dependence of the oscillation frequency obtained from the coherent phonon signal for the E_g mode observed in $LaAlO_3$. The solid curve describes the temperature dependence of the form $\omega \propto (T_c - T)^n$ with $n = 0.5$.

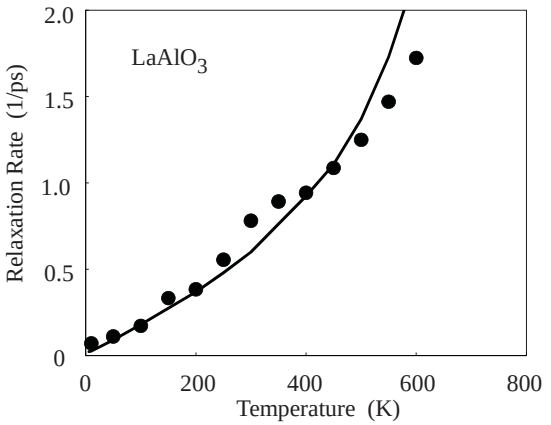

FIG. 9. Temperature dependence of the relaxation rate obtained from the coherent phonon signal for the E_g mode observed in $LaAlO_3$. The solid curve represents the theoretical curve including the frequency change obtained from Eq. (1) with $\gamma_0 = 2.3 \times 10^{10}$ s^{-1}; the observed phonon frequencies for the E_g mode in $LaAlO_3$ in Fig. 8 are used for each temperature.

materials, the relaxation process of the coherent phonon is considered to be dominated by the population decay due to the anharmonic phonon-phonon coupling[45–47] rather than by pure dephasing. According to the anharmonic decay model,[45] the relaxation of optical phonons in the center of the Brillouin zone is considered to occur through two types of decay process, namely the down-conversion process and the up-conversion process. In the down-conversion process, the initial ω_0 phonon with wave vector $k \simeq 0$ decays into two lower-energy phonons, ω_i and ω_j, with opposite wave vectors, k and $-k$; these lower-energy phonons belong to the i branch and j branch of the phonon. The energy and wave-vector conservations are given by $\omega_0 = \omega_{ik} + \omega_{j-k}$. In the up-conversion process, the initial excitation is scattered by a thermal phonon (ω_{ik}) into a phonon of higher energy (ω_{jk}), where $\omega_0 + \omega_{ik} = \omega_{jk}$. The down-conversion process can be realized either for $i = j$ (overtone channel) or for $i \neq j$ (combination channel), depending on the phonon band structure of the material, while the up-conversion process contains only the combination channel and has no overtone channel. The formation of the combination channel is less probable because it involves three frequencies of phonons and three phonon branches, and stringent limitations are imposed by the energy and wave-vector conservations. On the other hand, the formation of the overtone channel is more probable because it involves two phonon branches (optical and acoustic); the energy and wave-vector conservations are necessarily satisfied by two acoustic phonons with the same frequency and opposite wave vectors if the maximum frequency of the acoustic branch is greater than half the frequency of the initial optical phonon.

Here, we consider the down-conversion process in which an optical phonon decays into two acoustic phonons with half the frequency of the optical phonon and with opposite wave vectors. The temperature dependence of the relaxation rate γ of the coherent phonon is given by[45,46]

$$\gamma = \gamma_0 \left[1 + \frac{2}{\exp[(\hbar\omega_0/2)/k_B T] - 1} \right], \qquad (1)$$

where ω_0 is the frequency of the optical phonon and k_B is the Boltzmann constant.

In ordinary materials, the temperature dependence of the phonon frequency is small and the theoretical curve with a fixed value of the phonon frequency fits well to the experimental data. In the case of soft phonon modes, however, phonon frequencies change as the temperature is increased; in such a case, the frequency change must be considered. The solid curve in Fig. 9 shows the theoretical curve including the frequency change obtained from Eq. (1) with $\gamma_0 = 2.3 \times 10^{10}$ s^{-1}, where the observed phonon frequencies for the E_g mode in $LaAlO_3$ in Fig. 8 are used for each temperature. As observed in Fig. 9, the solid curve explains the experimental data well. In $LaAlO_3$, the observed relaxation for the soft-mode phonons is explained well by the population decay due to the anharmonic phonon-phonon coupling.

B. $KMnF_3$

The temperature dependence of the phonon frequency obtained from the coherent phonon signal observed in $KMnF_3$ is shown in Fig. 10. At temperatures below T_{cm}, three phonon modes were observed. From the result of the x-ray diffraction, Kapusta *et al.*[35] concluded that the low-temperature symmetry is monoclinic rather than orthorhombic and assigned the observed Raman lines to the monoclinic symmetries A_g and B_g. According to their assignment, the observed low-frequency phonon modes, whose frequencies are 0.8 and 1.2 THz at low temperatures, correspond to the $B_g(R)$ and $A_g(R)$ modes in the monoclinic phase; these modes originate from the tetragonal E_g soft mode and the cubic R mode. The higher-frequency phonon mode of 1.5 THz corresponds to the monoclinic $A_g(M)$ mode originating from the cubic M mode. Here, we refer to the observed three modes as the 0.8 THz mode, the 1.2 THz mode, and the 1.5 THz mode. In the Raman scattering experiments,[29,35] no soft-mode behavior was reported for the low-frequency modes. However, as shown in Fig. 10, slight but clear soft-mode behavior was observed in our experiment; the phonon frequencies of the three modes decrease as the temperature is

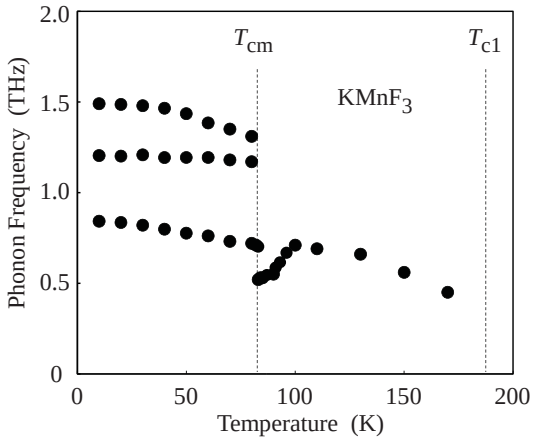

FIG. 10. Temperature dependence of the phonon frequency obtained from the coherent phonon signal observed in $KMnF_3$.

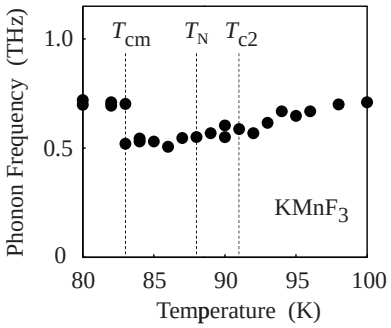

FIG. 11. Temperature dependence of the phonon frequency obtained from the coherent phonon signal observed between 80 and 100 K in $KMnF_3$.

increased toward the phase-transition temperature T_{cm}. The softening of the phonon mode is evident for the 0.8 and 1.5 THz modes but is less evident for the 1.2 THz mode. With increasing temperature, a sudden change in the phonon frequency was observed at 83 K. This change, shown in Fig. 10, and the stepped anomaly in birefringence, shown in Fig. 3, unambiguously demonstrate the first-order character of this phase transition at T_{cm}, contrary to the assertion of Hidaka *et al.*,[30] who attributed a second-order character to this transition.

Considering the selection rules for the stimulated Raman process, the coherent phonon signal of the monoclinic A_g mode is expected for both [100] and [110] pumping, while that of the monoclinic B_g mode is expected only for [110] pumping. This expectation is not consistent with the observed pumping-direction dependence shown in Fig. 4, if we assign the 0.8, 1.2, and 1.5 THz modes to the monoclinic $B_g(R)$, $A_g(R)$, and $A_g(M)$, respectively. The temperature dependence of the phonon frequency for the 0.8 THz mode in Fig. 10 is similar to that for the 1.5 THz mode. However, the temperature dependence of the phonon frequency for the 1.2 THz mode is different from that of the other two modes. It may be natural to consider that the 0.8 and 1.5 THz modes originate from the same cubic mode. Also, at this point, the monoclinic assignment is not probable. If we assign the 1.2 and 1.5 THz modes to $A_g(M)$ and $A_g(R)$, respectively, the 0.8 and 1.5 THz modes originate from the same cubic R mode. However, this assignment still does not explain the observed pumping-direction dependence.

Another candidate for the low-temperature symmetry is orthorhombic symmetry. In the orthorhombic symmetry, the 0.8, 1.2, and 1.5 THz modes are assigned to the orthorhombic $B_{1g}(R)$, $A_g(M)$, and $B_{2g}(R)$.[35] The coherent phonon signal of the orthorhombic A_g mode is expected only for [100] pumping, and the coherent phonon signals of the B_{1g} and B_{2g} modes are expected only for [110] pumping. This expectation is consistent with the observed pumping-direction dependence shown in Fig. 4 if orthorhombic assignment is employed. In addition, it is probable that the 0.8 and 1.5 THz modes originate from the same cubic R mode. The low-temperature symmetry of $KMnF_3$ is suggested to be orthorhombic from the observed pumping-direction dependence of the coherent phonon signal and the temperature dependence of the phonon frequencies in our experiment.

Small peaks, which are not expected from the selection rules for the orthorhombic symmetry, are also found in the Fourier spectra in Fig. 4(b): the 0.8 and 1.5 THz modes for the [100] pumping and the 1.2 THz mode for the [110] pumping. This may be caused by the inaccuracy in the direction of the pumping polarization, the incompleteness of the single crystal, or the breaking of the crystalline symmetry.[48] For the pumping pulse with the polarization direction between the [100] and [110] axes, coherent phonon signals for all three modes appear. It was observed that the changes in the spectral intensities of the 0.8 and 1.5 THz modes show a similar behavior for the direction change of the pump polarization; they increase together or decrease together. It was also observed that the change in the spectral intensity of the 1.2 THz mode shows an opposite behavior to the other modes, that is, increase and decrease. This fact also supports the orthorhombic assignment.

In the temperature range above T_{cm}, as shown in Figs. 6 and 7, a signal of relaxation type was observed for [100] pumping and a damped oscillation with a single frequency was observed for [110] pumping. The phonon frequency obtained from the coherent phonon signals for [110] pumping is plotted in Fig. 10. From Fig. 10, after the jump at T_{cm}, the frequency becomes larger in the temperature range between T_{cm} and 100 K, after which it is softened toward the phase-transition temperature T_{c1}. This soft phonon mode is considered to correspond to the tetragonal E_g mode.

The temperature dependence of the phonon frequency between 80 and 100 K is shown in greater detail in Fig. 11. At T_{cm}, the phonon frequency suddenly decreases and then increases monotonously as the temperature is increased up to 100 K. In our experiment, no anomaly is found at T_N and T_{c2}.

It is known that the phase transition at T_{c2} is induced by a condensation of the M-mode soft phonons in the cubic perovskite structure of $KMnF_3$. The condensation induces an in-phase tilt of MnF_6 octahedra about the [001] axis. In the x-ray diffraction experiment,[34] the lattice constants are not changed at T_{c2}. In the neutron diffraction experiment,[36] the weak reflection signal due to the M-mode condensation disappears at T_{c2} after decreasing largely around T_{cm}. However, it was suggested that there is a short-range order of the in-phase tilt of MnF_6 octahedra even above T_{c2}. These results

indicate that structural change does not abruptly occur at T_{c2} and that the M-mode condensation continues without any anomaly in the lattice constants. This is consistent with our experimental results; notable changes in birefringence and phonon frequency are observed at around 90 K, but no distinct anomaly is found at T_{c2}.

The selection rules for coherent phonon signals, which are generated through the process of impulsive stimulated Raman scattering, are the same as those for the usual Raman scattering signals. According to the selection rules, no Raman or coherent phonon signal is expected in the centrosymmetric cubic phase; however, two very broad bands were observed above T_{c1} in the Raman scattering experiments.[29,35] This unusual Raman activity in the cubic phase starts in the tetragonal phase. Its appearance was interpreted as a second-order Raman activity due to the existence of structural disorder in an averaged cubic symmetry.[35] This implies that lower-temperature local distortions remain considerably far above the phase-transition temperature T_{c1}. Structural disorder is related to the growth of quasielastic scattering, usually corresponding to a central peak in neutron scattering experiments. The coherent phonon signal of relaxation type observed at around T_{c1} in Fig. 6 is consistent with the observed unusual Raman activity,[29,35] neutron central peak,[26,49,50] and x-ray quasi-Bragg peak.[50]

The solid circles and squares in Fig. 12 show the temperature dependences of the relaxation rate obtained from the observed coherent phonon signals for the 0.8 and 1.2 THz modes below T_{cm} in $KMnF_3$; these modes are dominant in the signals for [110] and [100] pumping, respectively. The relaxation rates for both types of pumping increase with the temperature. The solid and broken curves in Fig. 12 represent the theoretical curves obtained from Eq. (1) with $\gamma_0 = 7 \times 10^{10}$ s^{-1} for the 0.8 THz mode and with 4×10^{10} s^{-1} for the 1.2 THz mode, respectively; the observed phonon frequencies for the 0.8 and 1.2 THz modes in $KMnF_3$ in Fig. 10 are used for each temperature. The theoretical curves explain the experimental data qualitatively, though the agreement between the experimental and theoretical results in the case of $KMnO_3$ is not as good as in the case of $LaAlO_3$.

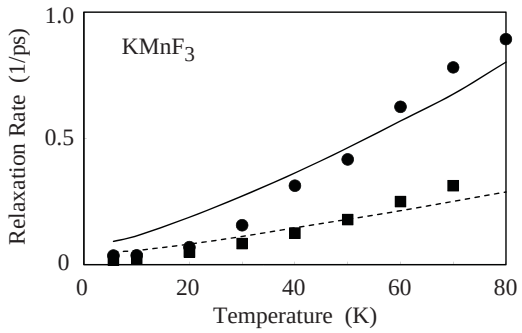

FIG. 12. Temperature dependence of the relaxation rate obtained from the coherent phonon signals below T_{cm} in $KMnF_3$. The solid circles and squares represent the relaxation rates for the 0.8 and 1.2 THz modes, respectively. The solid and broken curves represent the theoretical curves obtained from Eq. (1) with $\gamma_0 = 7 \times 10^{10}$ s^{-1} for the 0.8 THz mode and with 4×10^{10} s^{-1} for the 1.2 THz mode; the observed phonon frequencies for the 0.8 and 1.2 THz modes in $KMnF_3$ in Fig. 10 are used for each temperature.

V. SUMMARY

We have applied ultrafast polarization spectroscopy to observe the coherent phonons in two perovskite dielectrics, $LaAlO_3$ and $KMnF_3$, and showed that this approach in the time domain is very useful for the study of soft phonon modes. Coherent phonons are generated by linearly polarized pump pulses. The time-dependent linear birefringence induced by the generated coherent phonons is detected as a change in the polarization of the probe pulses. High detection sensitivity of $\sim 10^{-5}$ in the polarization change has been achieved in our detection system. Damped oscillations of coherent phonons were observed for several soft modes, which contribute to the structural phase transitions. The temperature dependences of the frequency and relaxation rate of the observed coherent phonons were measured, and the softening of the phonon frequencies was observed.

$LaAlO_3$ and $KMnF_3$ have the same perovskite crystal structure, and their structural phase transitions are related to the same rotation of the octahedra. However, the behaviors of the structural phase transitions in the two materials are considerably different. In $LaAlO_3$, a typical softening of the phonon frequency toward the phase-transition temperature T_c ($\sim$750 K) was observed. The temperature dependence of the phonon frequency is explained well by the classically expected relation $\omega \propto (T_c - T)^{1/2}$. The phonon relaxation is explained well by the decay model of the frequency-changing phonon, in which the optical phonon decays into two acoustic phonons due to anharmonic phonon-phonon coupling.

In $KMnF_3$, two structural phase-transition temperatures, T_{c1} (= 187 K) and T_{cm} ($\sim$81 K), are found in birefringence measurement. At temperatures below T_{cm}, three modes of coherent phonons were observed, and the phonon modes are found to undergo slight softening toward T_{cm}. Our experimental results of the pumping-direction dependence of the coherent phonon signal and the temperature dependence of the phonon frequencies suggest an orthorhombic structure at temperatures below T_{cm} instead of the monoclinic structure asserted by Kapusta *et al.*[35] through their x-ray diffraction experiment. At T_{cm}, the phonon frequency decreased suddenly, which indicates the first-order character of the phase transition. In the temperature range between T_{cm} and 100 K, notable changes were observed in the birefringence and phonon frequency. However, no distinct anomaly is found at T_{c2} (= 91 K) and T_N (= 88 K). This result suggests the existence of continuous change in the structure and is consistent with the x-ray[34] and neutron[36] diffraction experiments. In the temperature range between 100 K and T_{c1}, a softening of the E_g mode in the tetragonal symmetry is found toward T_{c1}. The coherent phonon signal of relaxation type appears at around T_{c1} and survives even at near room temperature. This signal suggests the existence of structural disorder in the cubic symmetry above T_{c1} and is consistent with the Raman scattering,[29,35] neutron scattering,[26,49,50] and x-ray diffraction[50] experiments.

It was shown that coherent phonon spectroscopy in the time domain is a very useful approach to studying the structural phase transitions and the soft phonon modes in dielectric materials.

[1]T. P. Dougherty, G. P. Wiederrecht, K. A. Nelson, M. H. Garrett, H. P. Jensen, and C. Warde, Science **258**, 770 (1992).
[2]H. J. Bakker, S. Hunsche, and H. Kurz, Rev. Mod. Phys. **70**, 523 (1998).
[3]W. G. Nilsen and J. G. Skinner, J. Chem. Phys. **48**, 2240 (1968).
[4]T. Kohmoto, K. Tada, T. Moriyasu, and Y. Fukuda, Phys. Rev. B **74**, 064303 (2006).
[5]Y. Koyama, T. Moriyasu, E. Okamura, Y. Yamada, K. Tanaka, and T. Kohmoto, Phys. Rev. B **81**, 024104 (2010).
[6]Y-X. Yan, E. B. Gamble Jr., and K. A. Nelson, J. Chem. Phys. **83**, 5391 (1985).
[7]G. A. Garrett, T. F. Albrecht, J. F. Whitaker, and R. Merlin, Phys. Rev. Lett. **77**, 3661 (1996).
[8]J. K. Kjems, G. Shirane, K. A. Muller, and H. J. Scheel, Phys. Rev. B **8**, 1119 (1973).
[9]J. F. Scott, Rev. Mod. Phys. **46**, 83 (1974).
[10]S. Geller and V. B. Bala, Acta Crystallogr. **9**, 1019 (1956).
[11]V. Plakhty and W. Cochran, Phys. Status Solidi **29**, K81 (1968).
[12]K. A. Muller, W. Berlinger, and F. Waldner, Phys. Rev. Lett. **21**, 814 (1968).
[13]C. de Rango, G. Tsoucaris, and C. Zelwer, C. R. Acad. Sci. (Paris) **259**, 1537 (1964).
[14]W. Cochran and A. Zia, Phys. Status Solidi **25**, 273 (1968).
[15]H. Thomas and K. A. Muller, Phys. Rev. Lett. **21**, 1256 (1968).
[16]J. F. Scott, Phys. Rev. **183**, 823 (1969).
[17]H. A. Klassens, P. Zalm, and F. O. Huysman, Philips Res. Rep. **8**, 441 (1953).
[18]A. Okazaki, Y. Suemune, and T. Fuchikami, J. Phys. Soc. Jpn. **14**, 1823 (1959).
[19]K. Hirakawa, K. Hirakawa, and T. Hashimoto, J. Phys. Soc. Jpn. **15**, 2063 (1960).
[20]O. Beckman and K. Knox, Phys. Rev. **121**, 376 (1961).
[21]A. J. Heeger, O. Beckman, and A. M. Portis, Phys. Rev. **123**, 1652 (1961).
[22]M. J. Cooper and R. Nathans, J. Appl. Phys. **37**, 1041 (1966).
[23]V. J. Minkiewicz and G. Shirane, J. Phys. Soc. Jpn. **26**, 674 (1969).
[24]G. Shirane, V. J. Minkiewicz, and A. Linz, Solid State Commun. **8**, 1941 (1970).
[25]V. J. Minkiewicz, Y. Fujii, and Y. Yamada, J. Phys. Soc. Jpn. **28**, 443 (1970).
[26]K. Gesi, J. D. Axe, G. Shirane, and A. Linz, Phys. Rev. B **5**, 1933 (1972).
[27]V. G. Khlyustov, I. N. Flerov, A. T. Silin, and A. N. Sal'nikov, Fiz. Tverd. Tela (Leningrad) **14**, 175 (1972) [Sov. Phys. Solid State **14**, 139 (1972)].
[28]Yu. A. Popkov, V. V. Eremenko, and V. I. Fomin, Fiz. Tverd. Tela (Leningrad) **13**, 2028 (1971) [Sov. Phys. Solid State **13**, 1701 (1972)].
[29]D. J. Lockwood and B. H. Torrie, J. Phys. C **7**, 2729 (1974).
[30]M. Hidaka, M. Ohama, A. Okazaki, H. Sakashita, and S. Yamakawa, Solid State Commun. **16**, 1121 (1975).
[31]H. Sakashita, N. Ohama, and A. Okazaki, J. Phys. Soc. Jpn. **50**, 4013 (1981).
[32]N. Akutsu and H. Ikeda, J. Phys. Soc. Jpn. **50**, 2865 (1981).
[33]U. J. Nicholls and R. A. Cowley, J. Phys. C **20**, 3417 (1987).
[34]A. Gibaud, S. M. Shapiro, J. Nouet, and H. You, Phys. Rev. B **44**, 2437 (1991).
[35]J. Kapusta, P. Daniel, and A. Ratuszna, Phys. Rev. B **59**, 14235 (1999).
[36]S. Watanabe, M. Yoshimura, M. Hidaka, and H. Yoshizawa, Appl. Phys. A **84**, 87 (2006).
[37]A. Salazar, M. Massot, A. Oleaga, A. Pawlak, and W. Schranz, Phys. Rev. B **75**, 224428 (2007).
[38]L. J. Lewis and Y. Lépine, Phys. Rev. B **40**, 3319 (1989).
[39]T. Kohmoto, Y. Fukuda, M. Kunitomo, and K. Isoda, Phys. Rev. B **62**, 579 (2000).
[40]R. V. Jones, Proc. R. Soc. London, Ser. A **349**, 423 (1976).
[41]T. Kohmoto, Y. Fukuda, and T. Hashi, Phys. Rev. B **34**, 6085 (1986).
[42]Y.-X. Yan and K. A. Nelson, J. Chem. Phys. **87**, 6257 (1987).
[43]Y. Liu, A. Frenkel, G. A. Garrett, J. F. Whitaker, S. Fahy, C. Uher, and R. Merlin, Phys. Rev. Lett. **75**, 334 (1995).
[44]K. Watanabe, N. Takagi, and Y. Matsumoto, Phys. Rev. Lett. **92**, 057401 (2004).
[45]F. Vallée, Phys. Rev. B **49**, 2460 (1994).
[46]M. Hase, K. Mizoguchi, H. Harima, S. I. Nakashima, and K. Sakai, Phys. Rev. B **58**, 5448 (1998).
[47]M. Hase, K. Ishioka, J. Demsar, K. Ushida, and M. Kitajima, Phys. Rev. B **71**, 184301 (2005).
[48]E. Matsubara, K. Inoue, and E. Hanamura, Phys. Rev. B **72**, 134101 (2005).
[49]S. M. Shapiro, J. D. Axe, G. Shirane, and T. Riste, Phys. Rev. B **6**, 4332 (1972).
[50]A. Gibaud, H. You, S. M. Shapiro, and J. Y. Gesland, Phys. Rev. B **42**, 8255 (1990).